Matheus de B. Vallim,[1] *José M. C. Dos Santos,*[2] *and Argemiro L. A. Costa*[3]

Motorcycle Analytical Modeling Including Tire–Wheel Nonuniformities for Ride Comfort Analysis

REFERENCE: Vallim, M. B., Dos Santos, J. M. C., and Costa, A. L. A., **"Motorcycle Analytical Modeling Including Tire–Wheel Nonuniformities for Ride Comfort Analysis,"** *Tire Science and Technology*, TSTCA, Vol. 45, No. 2, April–June 2017, pp. 101–120.

ABSTRACT: The transmission of vibrations in motorcycles and their perception by the passengers are fundamental in comfort analysis. Tire nonuniformities can generate self-excitations at the rotational frequency of the wheel and contribute to the ride vibration environment. In this work a multi-body motorcycle model is built to evaluate the ride comfort with respect to tire nonuniformities. The aim is to obtain a multi–degrees-of-freedom dynamic model that includes both the contributions of the motorcycle and tire–wheel assembly structures. This representation allows the tire nonuniformities to predict the vertical force variations on the motorcycle and can be used through a root mean square acceleration evaluation for ride comfort analysis. The motorcycle model proposed is a 10-degrees-of-freedom system, where each tire–wheel is a 4-degrees-of-freedom model. The tire–wheel assemblies include two types of nonuniformities: lumped mass imbalance and radial run-out. Simulations of analytical models are compared with experimental tests.

KEY WORDS: tire–wheel model, motorcycle model, motorcycle tire nonuniformity, radial run-out, lumped mass imbalance, ride comfort

Introduction

Two-wheeled vehicles are increasingly present on the roads because of their low prices, low fuel consumption, and facility of maintenance. As with cars and other vehicles, motorcycles also need attention with respect to ride characteristics and comfort.

Vehicle manufacturers have tried to reduce noise and vibration transmitted to occupants. Vibrations, usually generated by steering systems, engine, suspension, exhaust system, and tires, can cause discomfort and even the failure of mechanical components.

Vehicle, tire, and road can relate and generate "ride disturbances" through the air (airborne noise) or through the structure of tire and vehicle (structural borne vibrations) [*1*]. In this perspective, pneumatic tires can become an important source of vibration when tire–wheel assemblies have some degree of nonuniformity. Tire nonuniformities refer to material or

[1] Corresponding author. Faculty of Mechanical Engineering, 200 Rua Mendeleyv, Campinas, São Paulo, 13083-860, CP 6122, Brazil. Email: matheusvallim@gmail.com

[2] Faculty of Mechanical Engineering, 200 Rua Mendeleyv, Campinas, São Paulo, 13083-860, CP 6122, Brazil. Email: zema@fem.unicamp.br

[3] Pirelli Pneus Ltda, 871 Avenida Giovanni Battista Pirelli, Santo André, São Paulo, 09111-340, Brazil. Email: argemiro.costa@pirelli.com

manufacturing anomalies such as tire run-out, rim run-out, tire–bead area placement variations, and other bead-seating errors [*2*]. They can be mathematically represented as mass imbalance, geometric nonuniformities, and stiffness variations, which can induce varying forces that act on the axle of wheel. These forces are generated when the tire rolls with an angular velocity related to the velocity of the vehicle, creating oscillatory excitations that are transmitted through different structures of the vehicle.

Several works have been developed to investigate tire dynamic and tire vibrational behavior, vibration transmission from tire to vehicle, and the effects of nonuniformities on force generation at wheel spindle. Gong [*3*] modeled a tire as a flexible circular ring. The main objectives were to analyze the in-plane dynamics of tires and the vibration transmission properties of tire from road to the wheel. Dorfi [*4*] analyzed the force transmission through the tire structure by studying a tire rolling over cleats. An analytical approach determined natural frequencies and mode shapes based on traveling waves. A rigid ring model was also developed to study the fore/aft modes of the tire considering the effect of the footprint. Dorfi [*5,6*] also conducted some works of tire nonuniformities analysis. Tire analytical modelling, simulation, and experimental data were compared to study the force generation of tires nonuniformities and their influence on steering wheel vibrations. Dillinger [*7*] proposed tire–wheel analytical models to study tire nonuniformities based on a rigid ring connected to a disc with stiffness and damper elements. He analyzed the effects of mass imbalance and geometric imperfections. Stutts et al. [*8*] studied the effect of radial stiffness nonuniformity in a tire using a rigid ring model. The results showed that the force produced by the stiffness nonuniformity was parametric in nature, creating a possibility of a parametric resonance in the system.

Unlike studies of tires and cars, motorcycle studies are limited in literature. The analyses are concentrated in maneuverability, handling, stability, and performance in curves. Sharp [*9*] studied the motorcycle in free control and analyzed its stability. He divided the vehicle in two frames joined at the steering axis. Tires were represented by two rigid discs, making a single point with the ground. With the advance of computer technology, Sharp et al. [*10*] improved the previous model, including a new tire modeling, a new treatment of rear suspension, a steady-state equilibrium analysis, and a steering control evaluation. Focusing on ride comfort analysis, Cossalter et al. [*11*] proposed a frequency-domain approach for evaluating a motorcycle in straight-running displacement. He analyzed the motorcycle frequency response to excitations caused by road unevenness using a nonlinear numerical multi-body model. Indices of comfort were calculated according to human sensitivity.

For analyzing motorcycle dynamic behavior, it is important to highlight the types of mode shapes found in a motorcycle. “In-plane” modes refer to the frame, suspension, and wheel motion in the vertical plane, which are related to ride comfort and road-holding. “Out-of-plane” modes involve roll, yaw,

steering angle, and steering head lateral displacement, characteristics of vehicle stability and handling [*12*].

The purpose of this paper is to introduce a motorcycle model able to reproduce the influence of tire nonuniformities in ride comfort. This analysis focuses on the vertical dynamic of the motorcycle; longitudinal and lateral effects are not considered. The model is built based on a lumped parameter model presented by Cossalter [*12*] due to its capacity to simply represent all parts of the motorcycle. A tire representation is also added to simulate its dynamics when tire nonuniformities generate vibration during the ride and affect the comfort.

The analytical multi-body model has five rigid bodies, totaling 10 degrees of freedom. One body is called "sprung mass" and represents the chassis, engine, steering head, and rider. It is connected to two "unsprung masses" with elastic systems (front and rear suspensions). Each unsprung mass is modeled with two rigid bodies (a rigid ring and a disc, connected by springs and dampers) to represent a tire–wheel assembly, based on Dillinger [*7*]. Mass imbalance and run-out nonuniformities are inserted mathematically as an external excitation on the coordinates related to the rigid body movements of tires and wheels.

The ride comfort analysis is made by evaluating the effect of each nonuniformity on the vertical acceleration response on the saddle of the motorcycle. In addition, sprung mass root mean square (RMS) accelerations are compared with comfort limits proposed by ISO 2631:1978 standard [*13*], within a 1–80 Hz frequency range.

In fact, the model proposed here is widely used for cars and trucks, known as a "half-car model." However, particular parameters such as stiffness, mass, and moment of inertia can characterize the system like a motorcycle at least for in-plane analysis. Moreover, the modeling of unsprung masses is more refined when compared with that present in half-car models.

In terms of ride comfort and tire nonuniformities, Cossalter's work [*12*] analyzes the motorcycle dynamics with a simple representation of the tires, as Sharp [*9*] and Sharp et al. [*10*] do, but with different goals. Although these authors have worked with multi-body models, both of them were developed to focus mainly on longitudinal and lateral dynamics of motorcycles. Also, a tire–wheel model without the sprung mass representation cannot be used to analyze ride comfort in terms of human sensitivity; therefore, an assembly of the vehicle and tire representation should be proposed.

Since this motorcycle model is linear and not difficult to develop, it consumes less time in engineering analysis and can serve as a starting point for future works of ride comfort of motorcycles related to tire nonuniformities.

Motorcycle Model

Energy Formulation

The model proposed here is based on Cossalter [*12*], shown in Fig. 1.

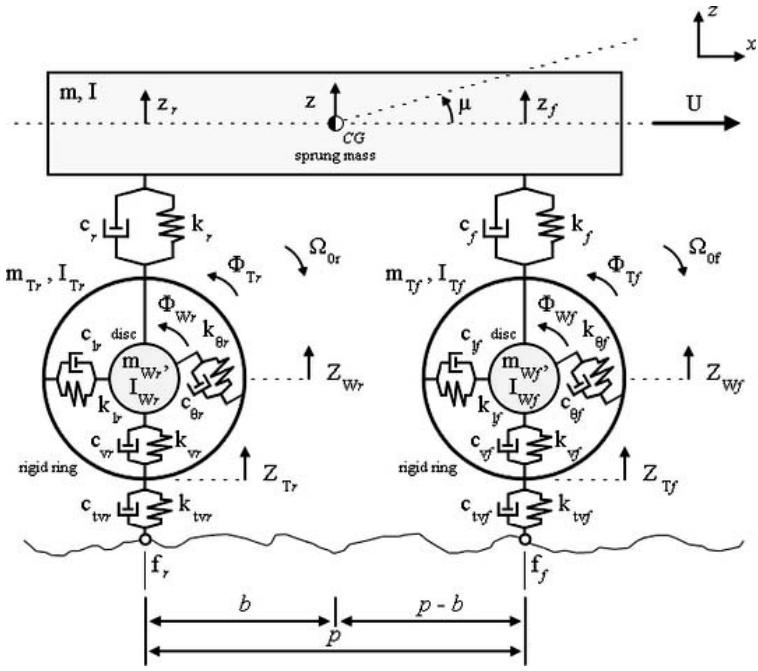

FIG. 1 — *10 DOF motorcycle model.*

It consists of a sprung mass connected to two discs by two vertical springs and damper elements, which represent the rear and front suspensions. Each disc represents one wheel of the motorcycle and is connected to one rigid ring by two radial springs (horizontal and vertical) and one torsional spring. These springs reproduce the tire sidewall stiffness and the stiffness caused by the tire internal pressure in radial and angular directions. In this model, the rigid rings are the two tires of the vehicle. A vertical spring is included between each rigid ring and the road to represent the tread stiffness of each tire. Damper elements are also placed in parallel with springs to constitute the damping behavior of the system.

This kind of representation is able to exhibit 10 mode shapes of the vehicle, including the modes of the tire and wheel systems. The vibratory behavior modeling is critical when nonuniformity force excitations are studied, because the transmission of forces and vibrations affects the system response according to its structural characteristics.

Some assumptions and simplifications need to be taken into account. All the coordinates of the system are independent. The sprung mass is modeled in its plane of symmetry and has only 2 degrees of freedom, z and μ, as indicated

in Fig. 1. Each tire–wheel assembly has 4 degrees of freedom, Φ_{Wi}, Φ_{Ti}, Z_{Wi}, and Z_{Ti}, where $i = r, f$, totaling 10 coordinates in the whole system. Based on Dillinger [7], the mass of tire sidewall is negligible, the damping is considered viscous, the springs are linear, and there is no slippage between the tires and the road. Also, the wheels rotate freely.

The model has one coordinate system, as indicated in the scheme by *xyz*. The vehicle moves forward with a velocity of U. The rear tire rotates with an angular velocity of $\Omega_{0r} = U/R_r$, while the front tire rotates with $\Omega_{0f} = U/R_f$. R_r and R_f are, respectively, the rear and front tire radius.

To formulate the equations of the system, Lagrange's formulation is used:

$$\frac{\partial}{dt}\left(\frac{\partial L}{\partial \dot{q}_n}\right) - \frac{\partial L}{\partial \dot{q}_n} + \frac{\partial F}{\partial \dot{q}_n} = Q_n, \tag{1}$$

where

$$L = T - V. \tag{2}$$

T is the kinetic energy of the system, represented by the sum from Eqs. (3) to (7), V is the potential energy, indicated from Eqs. (8) to (10), and F is the dissipated energy, shown in Eqs. (11) to (13). Q_n represents the excitations on the system, where n is the number of degrees of freedom.

Kinetic energy is given by

$$T_1 = \frac{1}{2} I_{Tr}(\Omega_{0r} - \dot{\Phi}_{Tr})^2 + \frac{1}{2} m_{Tr} \dot{Z}_{Tr}^2 + \frac{1}{2} m_{Tr}(\dot{\Phi}_{Tr} R_r)^2, \tag{3}$$

$$T_2 = \frac{1}{2} I_{Tf}(\Omega_{0f} - \dot{\Phi}_{Tf})^2 + \frac{1}{2} m_{Tf} \dot{Z}_{Tf}^2 + \frac{1}{2} m_{Tf}(\dot{\Phi}_{Tf} R_f)^2, \tag{4}$$

$$T_3 = \frac{1}{2} I_{Wr}(\Omega_{0r} - \dot{\Phi}_{Wr})^2 + \frac{1}{2} m_{Wr} \dot{Z}_{Wr}^2, \tag{5}$$

$$T_4 = \frac{1}{2} I_{Wf}(\Omega_{0f} - \dot{\Phi}_{Wf})^2 + \frac{1}{2} m_{Wf} \dot{Z}_{Wf}^2, \tag{6}$$

$$T_5 = \frac{1}{2} I \dot{\mu}^2 + \frac{1}{2} m \dot{z}^2. \tag{7}$$

Equations (3) to (7) represent, respectively, the kinetic energy of the rear tire, front tire, rear wheel, front wheel, and sprung mass. I_{Tr} and I_{Tf} are the mass moments of inertia of the rigid rings; I_{Wr} and I_{Wf} are the mass moments of inertia of the discs; m_{Tr} and m_{Tf} are the masses of the rigid rings; m_{Wr} and m_{Wf} are the masses of the discs; I is the mass moment of inertia of the motorcycle; and m is the mass of the sprung mass. The terms $(\Omega_{0i} - \Phi_{Ti})$ and

($\Omega_{0i} - \Phi_{Wi}$) represent the angular velocity of the rigid rings and discs, where $i = r, f$.

Potential energy can be written as follows:

$$V_1 = \frac{1}{2}k_{tvr}Z_{Tr}^2 + \frac{1}{2}k_{vr}(Z_{Wr} - Z_{Tr})^2 + \frac{1}{2}k_{lr}(\Phi_{Tr}R_r)^2 + \frac{1}{2}k_{\theta r}(\Phi_{Wr} - \Phi_{Tr})^2, \quad (8)$$

$$V_2 = \frac{1}{2}k_{tvf}Z_{Tf}^2 + \frac{1}{2}k_{vf}(Z_{Wf} - Z_{Tf})^2 + \frac{1}{2}k_{lf}(\Phi_{Tf}R_f)^2 + \frac{1}{2}k_{\theta f}(\Phi_{Wf} - \Phi_{Tf})^2, \quad (9)$$

$$V_3 = \frac{1}{2}k_r(z - b\mu - Z_{Wr} - Z_{Tr})^2 + \frac{1}{2}k_f\left[z + (p-b)\mu - Z_{Wf} - Z_{Tf}\right]^2. \quad (10)$$

Equations (8) and (9) represent the potential energy associated to stiffness elements of the tire–wheel assemblies. Equation (10) is the potential energy of the rear and front suspension. The parameters k_{tvr} and k_{tvf} are the vertical tread stiffness of the tires, k_{vr} and k_{vf} are the vertical stiffness of the tires, k_{lr} and k_{lf} are the horizontal stiffness of the tires, and $k_{\theta r}$ and $k_{\theta f}$ are torsional stiffness of the tires. Finally, k_r and k_f are the stiffness of rear and front suspension, respectively. The parameter p represents the motorcycle wheel-base, while b is the distance between the contact point of the rear tire to the center of gravity (CG) of motorcycle.

The energy dissipation of the system is

$$F_1 = \frac{1}{2}c_{tvr}\dot{Z}_{Tr}^2 + \frac{1}{2}c_{vr}(\dot{Z}_{Wr} - \dot{Z}_{Tr})^2 + \frac{1}{2}c_{lr}(\dot{\Phi}_{Tr}R_r)^2 + \frac{1}{2}c_{\theta r}(\dot{\Phi}_{Wr} - \dot{\Phi}_{Tr})^2, \quad (11)$$

$$F_2 = \frac{1}{2}c_{tvf}\dot{Z}_{Tf}^2 + \frac{1}{2}c_{vf}(\dot{Z}_{Wf} - \dot{Z}_{Tf})^2 + \frac{1}{2}c_{lf}(\dot{\Phi}_{Tf}R_f)^2 + \frac{1}{2}c_{\theta f}(\dot{\Phi}_{Wf} - \dot{\Phi}_{Tf})^2, \quad (12)$$

$$F_3 = \frac{1}{2}c_r(\dot{z} - b\dot{\mu} - \dot{Z}Wr - \dot{Z}Tr)^2 + \frac{1}{2}c_f\left[\dot{z} + (p-b)\dot{\mu} - \dot{Z}_{Wf} - \dot{Z}_{Tf}\right]^2. \quad (13)$$

Equations (11) and (12) represent the energy dissipation of the tires and wheels. Equation (13) represents the damping system in rear and front suspension in motorcycles, respectively. The parameters c_{tvr} and c_{tvf} are the vertical tread damping of the tires, c_{vr} and c_{vf} are the vertical damping of the tires, c_{lr} and c_{lf} are the horizontal damping of the tires, and $c_{\theta r}$ and $c_{\theta f}$ are the torsional damping of the tires. Finally, c_r and c_f are the damping of rear and front suspension, respectively.

Applying Eq. (1), the mathematical representation of the system becomes

$$[M]_{10x10}\{\ddot{q}\}_{10x1} + [C]_{10x10}\{\dot{q}\}_{10x1} + [K]_{10x10}\{q\}_{10x1} = \{Q\}_{10x1}, \quad (14)$$

where

$$\{q\}_{10x1} = \{\, \Phi_{Wr} \quad \Phi_{Tr} \quad Z_{Wr} \quad Z_{Tr} \quad \Phi_{Wf} \quad \Phi_{Tf} \quad Z_{Wf} \quad Z_{Tf} \quad z \quad \mu \,\}^T. \tag{15}$$

Equation (14) is a linear second order differential equation, where the vector $\{Q\}_{10x1}$ is the excitation imposed on the system (in this case, null). Nonuniformities are inserted in each tire–wheel assembly and mathematically represented as an external excitation.

Proceeding with the motorcycle dynamics analysis, it is worthwhile to develop the in-plane frequency response function (FRF) of the vehicle. It is defined as the ratio between the bounce and pitch accelerations amplitude of the sprung mass and the displacement of the contact point of the tires with the ground versus frequency [*12*]. For $j = -1^{1/2}$, it can be expressed as [*11*]:

$$[H]_{10x2} = \begin{bmatrix} H_{\ddot{\Phi}_{Wr},f_r} & H_{\ddot{\Phi}_{Wr},f_f} \\ H_{\ddot{\Phi}_{Tr},r} & H_{\ddot{\Phi}_{Tr},f_f} \\ H_{\ddot{Z}_{W_r},f_r} & H_{\ddot{Z}_{Wr},f_f} \\ H_{\ddot{Z}_{Tr},f_r} & H_{\ddot{Z}_{Tr},f_f} \\ H_{\ddot{\Phi}_{Wf},f_r} & H_{\ddot{\Phi}_{Wf},f_f} \\ H_{\ddot{\Phi}_{Tf},f_r} & H_{\ddot{\Phi}_{Tf},f_f} \\ H_{\ddot{Z}_{W_f},f_r} & H_{\ddot{Z}_{W_f},f_f} \\ H_{\ddot{Z}_{T_f},f_r} & H_{\ddot{Z}_{T_f},f_f} \\ H_{\ddot{z},f_r} & H_{\ddot{z},f_f} \\ H_{\ddot{\mu},f_r} & H_{\ddot{\mu},f_f} \end{bmatrix} = -\omega^2(-\omega^2[M] + j\omega[C] + [K])^{-1}(j\omega[C'] + [K']), \tag{16}$$

where

$$[C']_{10x2} = \begin{bmatrix} 0 & 0 & 0 & c_{tvr} & 0 & 0 & 0 & 0 & 0 & 0 \\ 0 & 0 & 0 & 0 & 0 & 0 & 0 & c_{tvf} & 0 & 0 \end{bmatrix}^T, \tag{17}$$

$$[K']_{10x2} = \begin{bmatrix} 0 & 0 & 0 & k_{tvr} & 0 & 0 & 0 & 0 & 0 & 0 \\ 0 & 0 & 0 & 0 & 0 & 0 & 0 & k_{tvf} & 0 & 0 \end{bmatrix}^T. \tag{18}$$

The terms of matrix $[H]_{10x2}$ represent the FRF of each system coordinate to the input in the tires, f_r and f_f. Equation (19) shows the FRF of the sprung mass considering the wheelbase filtering phenomenon [*11*]:

$$H\ddot{z} = H_{\ddot{z},fr}e^{-j\omega(p/U)} + H_{\ddot{z},f_f}. \tag{19}$$

Model Verification

In order to verify the computational code of the motorcycle model, the frequency response on the saddle of the motorcycle was qualitatively compared with another multi-body Cossalter's model [*11*], based on Eq. (19), as shown in Fig. 2.

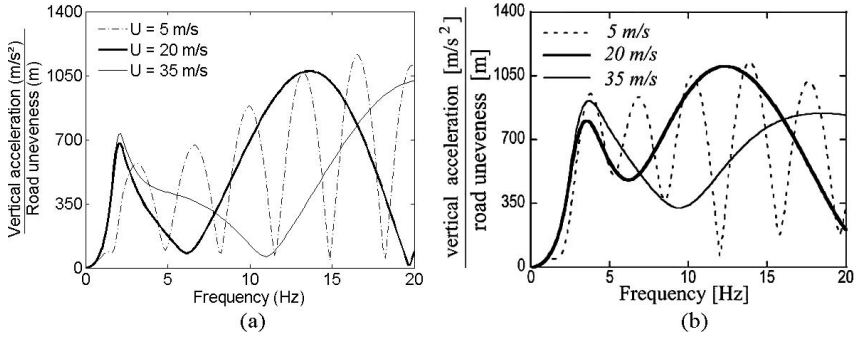

FIG. 2 — *Saddle vertical acceleration of (a) motorcycle model, (b) reference model [11].*

Although this Cossalter's model [*11*] is a nonlinear numerical model built to analyze the influences of road unevenness, the correlation between the two models is good. This comparison proves that the model developed is able to represent the vibration transmitted across its structure. Differences of amplitudes are due to the particularities of the system, since the natural frequencies affect the dynamic response. In addition, Eq. (19) shows that the response of the vehicle is modulated with a frequency U/p due to the imaginary exponential term. This represents the wheelbase filtering of the vehicle, that is, the time delay that the rear tire is excited after the front one.

Mass Imbalance

As previously commented, tire nonuniformities are related to anomalies generated during the manufacturing process. The mass imbalance phenomenon appears when there is a mass distribution concentrated on a single point.

The mass imbalance effect is taken into account when a single point of mass is inserted in a tire–wheel assembly, as shown in Fig. 3. The mathematical approach to the phenomenon for the whole motorcycle analytical system is described in Eq. (20), based on Dillinger [*7*] and Stutts et al. [*14*]:

$$\{Q\}_{10x1} = \{0 \quad T_{mr} \quad 0 \quad F_{mr} \quad 0 \quad T_{mf} \quad 0 \quad F_{mf} \quad 0 \quad 0\}^T, \tag{20}$$

where, for $i = r, f$,

$$T_{mi} = m_{imb\_i} R_i^2 \Omega_{0i}^2 \sin(\Omega_{0i} t + \theta_{imb\_i}), \tag{21}$$

$$F_{mi} = -m_{imb\_i} R_i \Omega_{0i}^2 \cos(\Omega_{0i} t + \theta_{imb\_i}). \tag{22}$$

In this representation, m_{imb_r} and m_{imb_f} are the masses concentrated in the tires; θ_{imb_r} and θ_{imb_f} are the angular positions in rear and front tires, respectively.

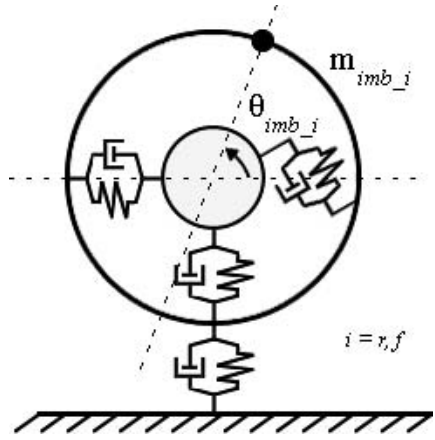

FIG. 3 — *Tire mass imbalance model.*

Run-out: Eccentricity

For geometric variation analysis, it is important to highlight that both stiffness nonuniformity and run-out imperfections belong to geometric variation class. Stiffness variation is due to geometric imperfections such as ply overlap, splices, and other dimensional aspects [*5*]. Run-out also belongs to geometric variations class. In addition, it is important to note that the tire acts like a spring in the radial direction. According to Dorfi [*5*], this "spring" can vary both in stiffness (stiffness variation) and in length (radial run-out). In this model, stiffness and geometry are considered uncoupled, and only run-out is evaluated to simplify the mathematical analysis.

Two types of run-out nonuniformity are evaluated. The first run-out representation considers a tire rolling with an eccentricity; that is, there is an offset between the geometric center of the tire and the center of rotation. The eccentricity mathematical model is represented in Fig. 4 and can be modeled in terms of an equivalent displacement [*14*]:

$$z_{ei} = Z_{ei}\cos(\Omega_{0i}t - \alpha_i), \tag{23}$$

where Z_{ei} is the eccentricity of rear and front tires and α_i is the angular positions where the eccentricity is maximum, for $i = r, f$.

This representation modifies the potential and dissipated energies of rear and front treads of the tires, which causes an addition in vector $\{Q\}_{10x1}$ from Eq. (14):

$$\{Q\}_{10x1} = \begin{Bmatrix} 0 & 0 & 0 & F_{\text{eccentricity}-r} & 0 & 0 & 0 & F_{\text{eccentricity}-f} & 0 & 0 \end{Bmatrix}^T, \tag{24}$$

where, for $i = r, f$,

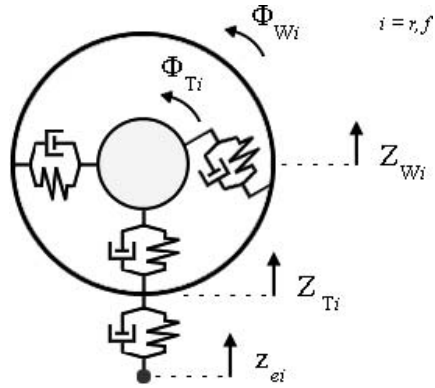

FIG. 4 — *Tire eccentricity model.*

$$F_{\text{eccentricity}-i} = k_{tvi} z_{ei} + c_{tvi} \dot{z}_{ei}. \tag{25}$$

Run-out: Out-of-Roundness

The second run-out model is based on Deodhar [*15*]. It consists of a tire with an elliptical shape (out-of-roundness), as seen in Fig. 5. In this representation, the tires have a semimajor axis a_i, a semiminor axis b_i, and a radius r'_i varying in function of $\Omega_{0i}t$, where $i = r, f$.

The radius variation can be defined as

$$\Delta Ri = \sqrt{\frac{a_i^2 b_i^2}{b_i^2 \cos^2(\Omega_{0i}t) + a_i^2 \sin^2(\Omega_{0i}t)}} - b_i, \tag{26}$$

where ΔRi defines the radial run-out of a tire in terms of an elliptical shape parameters, for $i = r, f$.

Owing to the representation as an elliptical shape, Deodhar [*15*] concluded that $\Delta Ri(t)$ oscillates with a frequency twice the angular velocity of the wheel.

The total force due to out-of-roundness representation can be modeled as the sum of radial force (product of tire vertical stiffness and the amplitude of the radius variation) and the imbalance centrifugal force due to run-out (product of mass tire, radius variation amplitude, and angular velocity squared) [*15*,*16*]. Therefore, the excitation vector $\{Q\}_{10x1}$ becomes

$$\{Q\}_{10x1} = \{0 \quad 0 \quad 0 \quad F_{\text{out}-\text{of}-\text{roundness}-r} \quad 0 \quad 0 \quad 0 \quad F_{\text{out}-\text{of}-\text{roundness}-f} \quad 0 \quad 0\}^T, \tag{27}$$

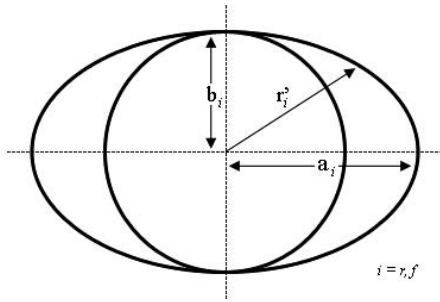

FIG. 5 — *Tire out-of-roundness model.*

where, for $i = r, f$,

$$F_{\text{out}-\text{of}-\text{roundness}-i} = k_{vi}\Delta R_i + m_{Ti}\Delta R_i \Omega_{0i}^2. \tag{28}$$

Motorcycle Physical Properties

The motorcycle analytical model of this project is based on a motorcycle provided by Pirelli Pneus Ltda for experimental tests. The rear tire is a 130/80-17 M/C 65S Tourance, attached to a rim 6.98 × 43.18 cm (2.75 × 17 inches), and the front tire is a 90/90-21M/C 54V TL MT90 Front A/T, attached to a rim 4.7 × 53.34 cm (1.85 × 21 inches). Both are bias tires.

The parameter values for tires and wheels were obtained by Pirelli Pneus Ltda. No damping parameter values are considered because they demand time and cost to be defined. Mass moments of inertia of the rigid rings are the mass moments of inertia of the tires, acquired by Abaqus® simulations. Mass moments of inertia of the discs are the mass moments of inertia of the wheels, established in a computer aided design (CAD) software. Torsional stiffness was obtained in Abaqus by measuring the angular displacement of the sidewall of each tire after having applied a moment. A radial equivalent stiffness k_{eq} was measured by pressing the tire to the ground. Owing to the difficulty to determine the tread stiffness, it approached 1,500,000 N/m, based on the values used by Dillinger [7]. Radial stiffness values k_{vi} and k_{li} were determined considering that k_{eqi} is the equivalent stiffness of k_{vi} and k_{tvi} disposed in series, as shown in Fig. 1 and in Eq. (29), where $i = r, f$:

$$k_{eqi} = \frac{k_{vi}k_{tvi}}{k_{vi} + k_{tvi}}. \tag{29}$$

For the rear tire–wheel assembly, the mass moment of inertia of the disc, I_{Wr}, is 0.2063 kg m^2; the mass moment of inertia of the rigid ring, I_{Tr}, is 0.593 kg m^2; the disc mass, m_{Wr}, is 7.5 kg; the rigid ring mass, m_{Tr}, is 6.1 kg; the rigid

ring radius, R_r, is 0.3249 m; the torsional stiffness of the tire, $k_{\theta r}$, is 11,800 N m/rad; the radial equivalent stiffness of the tire, k_{eqr}, is 127,000 N/m; the vertical stiffness and longitudinal stiffness of the tire, k_{vr} and k_{lr}, respectively, are 138,750 N/m; and the vertical tread stiffness of the tire, k_{tvr}, is 1,500,000 N/m.

For the front tire–wheel assembly, the mass moment of inertia of the disc, I_{Wf}, is 0.2679 kg m^2; the mass moment of inertia of the rigid ring, I_{Tf}, is 0.491 kg m^2; the disc mass, m_{Wf}, is 6.5 kg; the rigid ring mass, m_{Tf}, is 4.29 kg; the rigid ring radius, R_f, is 0.3513 m; the torsional stiffness of the tire, $k_{\theta f}$, is 13,600 N m/rad; the radial equivalent stiffness of the tire, k_{eqf}, is 122,000 N/m; the vertical stiffness and longitudinal stiffness of the tire, k_{vf} and k_{lf}, respectively, are 132,800 N/m; and the vertical tread stiffness of the tire, k_{tvf}, is 1,500,000 N/m.

Pirelli Pneus Ltda also provided some motorcycle parameters, like the mass of motorcycle plus the rider, M, and the loads on wheels under statistic condition, N_{Sr} and N_{Sf} (considering the rider on the vehicle). Suspensions damping and stiffness values were established based on Cossalter [*12*].

Longitudinal distance b was obtained as follows [*12*]:

$$b = \frac{N_{Sf}p}{M} = p - \frac{N_{Sr}p}{M}. \tag{30}$$

Sprung mass m is defined as the mass of the components above the suspensions and tire–wheel assemblies, like chassis, engine, and rider. Thus, it can be expressed as

$$m = M - (m_{Wr} + m_{Tr} + m_{Wf} + m_{Tf}). \tag{31}$$

Finally, the motorcycle mass moment of inertia including the rider was calculated multiplying the rider mass, m_{rd}, by an approximated pitch gyration radius of the rider, r_{rd}, plus the sprung mass, m, by an approximated pitch gyration radius of the motorcycle, r_m, expressed as

$$I = m_{rd}r_{rd}^2 + mr_m^2. \tag{32}$$

According to Cossalter [*12*], the pitch gyration radius value of a motorcycle is between 0.45 and 0.55 m and, per rider, is between 0.23 to 0.28 m.

Therefore, for the whole motorcycle model, the mass of motorcycle plus the rider, M, is 257 kg; the mass of sprung mass, m, is 232.61 kg; the rider mass, m_{rd}, is 72 kg; the motorcycle pitch gyration radius, r_m, is estimated to 0.50 m; the rider pitch gyration radius, r_{rd}, is estimated to 0.25 m; the motorcycle mass moment of inertia, I, is calculated to 62.653 kg m^2; the wheel-base, p, is 1.505 m; the longitudinal distance, b, is 0.63245 m; the load on the rear wheel, N_{Sr}, is 149 kg; the load on the front wheel, N_{Sf}, is 108 kg; the rear suspension stiffness, k_r, is 24,000 N/m; the front suspension stiffness, k_f, is 15,000 N/m; the rear suspension damping, c_r, is 750 N s/m; and the front suspension damping, c_f, is 500 N s/m.

TABLE 1 — *Motorcycle model natural frequencies and mode shapes.*

Mode	Value (Hz)	Description
1st	1.87	Motorcycle bounce
2nd	2.67	Motorcycle pitch
3rd	15.80	Torsional rear tire and wheel (in phase)
4th	17.40	Torsional front tire and wheel (in phase)
5th	22.85	Vertical displacement of rear wheel
6th	23.28	Vertical displacement of front wheel
7th	41.64	Torsional rear tire and wheel (in opposite phase)
8th	41.70	Torsional rear tire and wheel (in opposite phase)
9th	83.27	Vertical displacement of rear tire
10th	98.81	Vertical displacement of front tire

Results and Discussion

The motorcycle analytical model was implemented in a Matlab® computational code. Table 1 shows the natural frequencies and modes description of the vehicle. Modal analysis is important to predict the system dynamic behavior under resonance phenomena. Since nonuniformity excitations are predominately harmonics, there are some frequency ranges where ride comfort can be affected by amplitude amplifications of system response.

The first analysis includes accelerations evaluation on the sprung mass, where each nonuniformity is separately inserted in the model and analyzed. After that, RMS acceleration values are investigated to compare with comfort limits proposed by ISO 2631:1978 [*13*]. Finally, the model is compared with experimental tests.

Nonuniformities Evaluation

Nonuniformities evaluation was performed for $U = 50$, 80, and 120 km/h, typical velocities of a vehicle, observing the acceleration in time domain response on the sprung mass ($\ddot{z}$). It is important to focus on acceleration analysis because the human body is sensitive to accelerations, since they are correlated with amplitude of forces.

Sprung mass acceleration responses are shown in Figs. 6 to 8. Three situations were analyzed: a mass imbalance of $m_{imb\_f} = 100$ and 200 g in the front tire, shown in Fig. 6; a run-out of $z_{ef} = 1$ and 2 mm in the front tire, shown in Fig. 7; and a tire out-of-roundness for $a_f = 353.06$ mm ($1.005R_f$), $b_f = 351.3$ mm (R_f), and for $a_f = 354.81$ mm ($1.01R_f$), $b_f = 351.3$ mm (R_f), shown in Fig. 8.

As expected, Fig. 6 shows that the amplitude increases with velocity and mass. This increment, analyzed for the velocity, is a function of the angular velocity squared, in accordance with Eqs. (21) and (22). This explains why, for $U = 50$ km/h, the amplitude is very low.

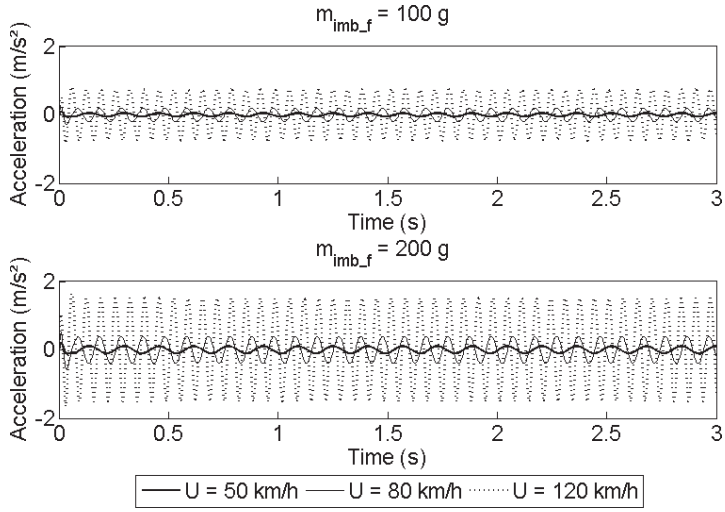

FIG. 6 — *Sprung mass time domain response for mass imbalance analysis.*

Figure 7 shows that the amplitude increases with run-out magnitude and velocity, but this increment is less sensitive with the velocity, different than observed in mass imbalance analysis.

Finally, the front tire out-of-roundness behavior is shown in Fig. 8. As discussed before, it is possible to see that it creates a second harmonic excitation, that is, the frequency imposed on the system corresponds to twice the

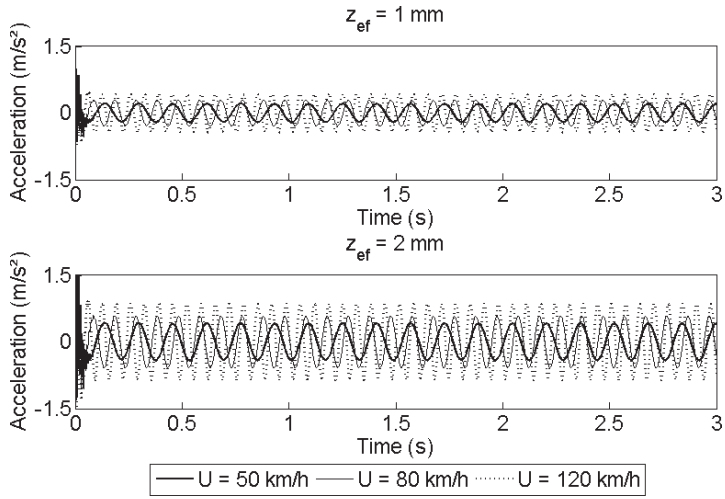

FIG. 7 — *Sprung mass time domain response for eccentricity nonuniformity.*

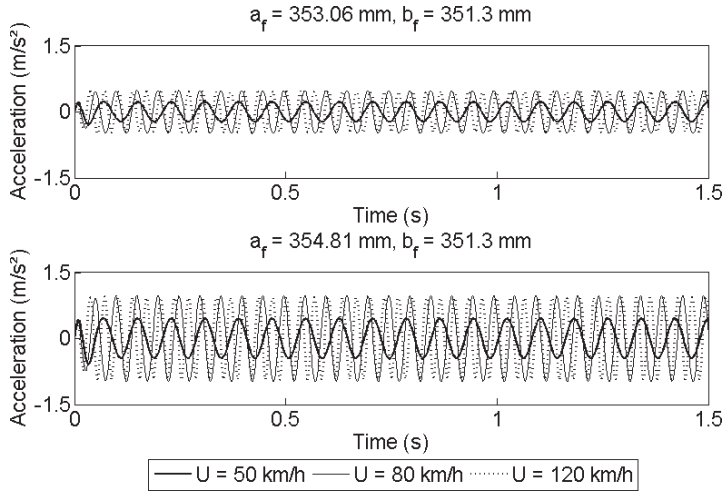

FIG. 8 — *Sprung mass time domain response for out-of-roundness nonuniformity.*

tire angular frequency. It can also be noted that the amplitudes related to $U = 80$ km/h and 120 km/h are very near. This is because, for $U = 80$ km/h, the frequency excitation (20.14 Hz) is near to the first vertical frequencies of wheels (22.85 Hz and 23.28 Hz), shown in Table 1. And, for $U = 120$ km/h, the amplitude keeps increasing, since the motorcycle velocity also increases.

Comfort Limits Analysis

In order to evaluate the ride comfort due to the tire nonuniformities, ISO 2631:1978 standard was used. It proposes an RMS acceleration analysis of the sprung mass spectrum comparing with comfort limits. The RMS accelerations are evaluated in one-third octave bands from 1 to 80 Hz, as pointed out by Griffin [*17*]. This means that the standard obtains many RMS values of an acceleration signal, one for each one-third octave band of the spectrum. Owing to the fact that the tire nonuniformities create, separately, excitations with only one frequency, a RMS value was taken only for its correspondent frequency band.

Figure 9 shows the RMS accelerations as a function of the front tire nonuniformities and the frequency of excitation and the "reduce comfort boundaries" proposed by the ISO 2631 standard.

It is possible to see in Fig. 9 the influence of each tire nonuniformity and the velocity to the comfort felt by the rider. For 50 km/h, the front tire with an eccentricity of 2 mm is between the 2.5 and 4 hour boundary comfort limit, that is, after riding for this amount of time, this nonuniformity causes discomfort on the saddle of the motorcycle. For 80 km/h, the 2 mm eccentricity and the tire out-of-roundness nonuniformity with a semimajor axis a_f of 354.8 mm have the

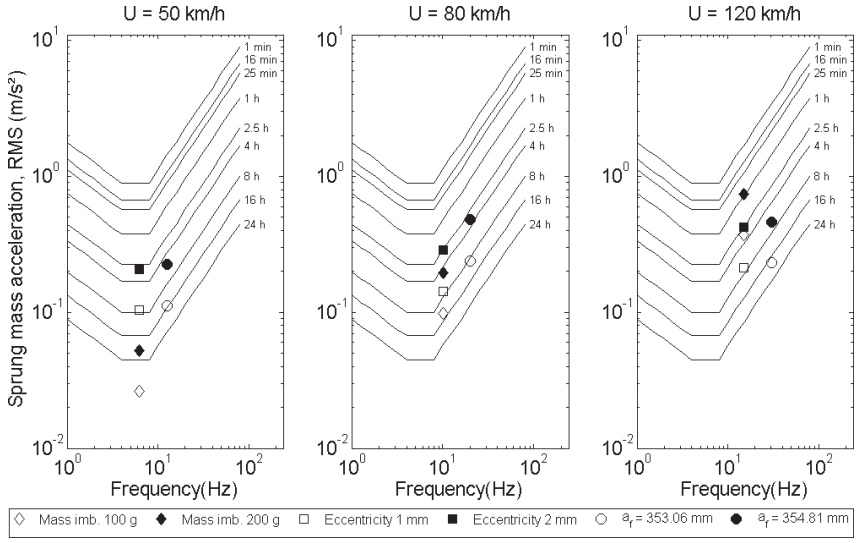

FIG. 9 — *ISO 2631 reduced comfort boundaries and sprung mass acceleration RMS.*

highest levels of discomfort (between 2.5 and 4 hours of exposure time). For 120 km/h, 200 g of mass imbalance has a significate level of vibration, which becomes uncomfortable for a ride of 1 hour.

Experimental Tests

The motorcycle model was compared with experimental tests realized by Pirelli Pneus Ltda. First, the motorcycle rode over a smooth road with a mass imbalance of 180 g in the front tire, for 80 km/h. After that, the same test was conducted without the mass imbalance. Measurements of acceleration were performed in the points A (rear wheel), B (rear suspension), C (engine), D (front suspension), and E (front wheel), shown in Fig. 10.

Figure 11 shows the results of the experimental tests for the points D (front suspension) and E (front wheel) and the analytical model results in the correspondent points $\ddot{z}_f$ (front suspension), given by Eq. (33), and $\ddot{Z}_{Wf}$ (front wheel), from Eq. (15).

$$\ddot{z}_f = \ddot{z} + (p - b)(\ddot{\mu}\cos\mu - \dot{\mu}2\sin\mu). \tag{33}$$

The experimental data obtained for the points D (front suspension) and E (front wheel), in Fig. 11a, show two tests: one with mass imbalance and another without the nonuniformity. It is possible to see the presence of a peak in 10 Hz for both points D and E (numerated as 1). This means that there is a source of excitation in this frequency on the vehicle, which can be due to tire nonuniformity. When a 180 g mass imbalance is added in the front tire, this

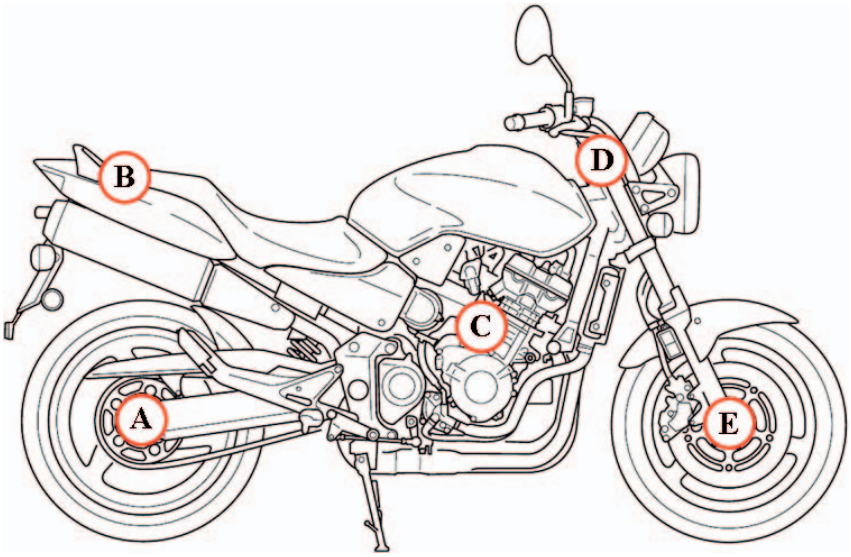

FIG. 10 — *Points of measurements for the experimental tests on the motorcycle.*

peak increases on the front wheel, but it remains practically constant on the front suspension.

Figure 11b shows the results for motorcycle analytical model simulations. When evaluated only with an eccentricity of 2 mm in the front tire, the model shows a peak in the front suspension response and in the front wheel response also in 10 Hz (represented as 1′). Adding a 180 g mass imbalance

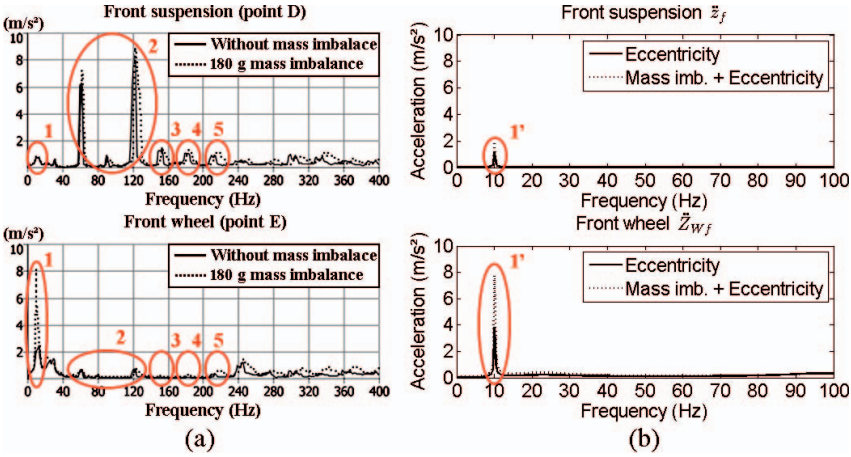

FIG. 11 — *(a) Motorcycle experimental tests. (b) Motorcycle analytical model simulations.*

FIG. 12 — *First three vertical mode shapes of the front tire.*

nonuniformity in phase with eccentricity in the front wheel, the amplitude of the front wheel reaches almost 8 m/s^2, near the value observed in experimental analysis for the point E. So, it is possible to guess the presence of tire eccentricity nonuniformity in the real motorcycle analyzed.

Figure 11a also shows other tire behaviors. The peaks located around 60 Hz and 120 Hz, indicated by the number 2, have high magnitudes on front suspension and are lower in the front wheel center. Since the engine excites the structure above the suspension, these peaks could be from the engine vibration. In this case, the damper system would be absorbing these excitations, being lower in the front wheel. In the case of the peaks numbered from 3 to 5, they could be correlated with some natural frequencies and mode shapes in the vertical direction, shown in Fig. 12.

A modal analysis was performed by Pirelli Pneus Ltda for the front tire under a preload N_{Sf} (defined previously) with an analytical wheel without mass. As seen in Fig. 12, the peaks from 3 to 5 possibly arise from the tire vibration related to its mode shapes, which is transmitted through the vehicle structure. However, in this case, it should be noted that the suspension could be amplifying these frequencies, since they are very small in the front wheel and very high on the front suspension, as shown in Fig. 11a.

Conclusions

The 10 DOFs motorcycle model proposed is capable of representing the tire nonuniformities of a motorcycle. Tire–wheel assemblies can be accommodated to easily receive geometric nonuniformities and mass imbalance modeling, since springs, damper elements, mass single points, and run-out positions can be placed according to the polar coordinate system of the tire. Furthermore, a 10 degrees-of-freedom system has a low computational cost, being easily modeled if compared with other complex methods. Also, it can be used as an important tool in the early stages of motorcycle tire design.

When tire nonuniformities are evaluated, the acceleration response on sprung mass depends of the type of nonuniformity and the motorcycle velocity.

As discussed before, these velocities are related to angular velocity of the wheels. Moreover, the type of nonuniformity influences the degree of harmonic excitation, contributing to different frequencies of excitation, which can affect ride comfort.

As a specific kind of comfort analysis, RMS acceleration evaluation is capable of verifying whether a nonuniformity will cause a discomfort or not, in function of the vehicle velocity and the exposure time.

This model meets the proposed requirement of being capable of analyzing how the occupants feel the disturbances caused by tire nonuniformities. The RMS analysis has only been applied due to a particular characteristic of this model: the representation of sprung mass, which includes the saddle and other components of the motorcycle structure. Also, the tire–wheel modeling allows the application of some tire physical properties, which can be used for sensitivity and optimization analysis for ride comfort on the motorcycle.

Finally, the comparison with experimental data showed that the model can predict the response related to a particular nonuniformity and seems to be satisfactory to other tire nonuniformities.

For future works, some actions can be taken to improve the model. Representing more motorcycle parts and, consequently, increasing the number of degrees of freedom can add more natural frequencies and mode shapes to the structure, improving the vibratory and dynamic behavior of the vehicle. In addition, a flexible ring model is capable of representing other ring modes and, consequently, other tire modes. In terms of comfort analysis, including the effect of the saddle structure as a vibration absorber and the RMS acceleration analysis on the handlebar can make the model more applicable for engineering analysis.

Acknowledgments

The authors would like to thank Pirelli Pneus Ltda and the University of Campinas for the support.

References

[*1*] Marshall, K. D., "Tire Noise and Vibration," *The Pneumatic Tire*, U.S. Department of Transportation, National Highway Traffic Safety Administration, Washington DC, 2006.

[*2*] Pottinger, M. G., "Uniformity: A Crucial Attribute of Tire/Wheel Assemblies," *Tire Science and Technology*, Vol. 38, 2010, pp. 24–46.

[*3*] Gong, S., "A Study of In-Plane Dynamics of Tires," M.Sc. Thesis, Delft University of Technology, Delft, 1993.

[*4*] Dorfi, H. R., "A Study of the In-Plane Force Transmission of Tires," *Tire Science and Technology*, Vol. 32, 2004, pp. 188–213.

[*5*] Dorfi, H. R., "Tire Non-Uniformities and Steering Wheel Vibrations," *Tire Science and Technology*, Vol. 33, 2005, pp. 64–102.

[*6*] Dorfi, H. R., "Tyre Non-Uniformities: Comparison of Analytical and Numerical Tyre Models and Correlation to Experimentally Measured Data," *Vehicle System Dynamics: International Journal of Vehicle Mechanics and Mobility*, Vol. 43, 2005, pp. 223–240.

[*7*] Dillinger, B. L., "The Development of Analytical Tire Models with Stiffness Non-Uniformity, Mass Imbalance, and Radial Run-out," M.Sc. Thesis, Clemson University, SC, 2005.

[*8*] Stutts, D. S, Krousgrill, C. M., and Soedel, W., "Parametric Excitation of Tire-Wheel Assembles by a Stiffness Non-Uniformity," *Journal of Sound and Vibration*, Vol. 179, 1995, pp. 499–512.

[*9*] Sharp, R. S., "The Stability and Control of Motorcycles," *Journal Mechanical Engineering Science*, Vol. 13, 1971, pp. 316–329.

[*10*] Sharp, R. S., Evangelou and Limebeer, D. J. N., "Advances in the Modelling of Motorcycle Dynamics," *Multibody System Dynamics*, Vol. 12, 2004, pp. 251–283.

[*11*] Cossalter, V., Doria, A., Garbin, S., and Lot, R., "Frequency-Domain Method for Evaluating the Ride Comfort of a Motorcycle," *Vehicle System Dynamics: International Journal of Vehicle Mechanics and Mobility*, Vol. 44, April 2006, pp. 339–355.

[*12*] Cossalter, V., *Motorcycle Dynamics*, 2nd English ed., Lulu, Raleigh, NC, 2006.

[*13*] International Standards Organization, ISO 2631:1978, "Guide for the Evaluation of Human Exposure to Whole-Body Vibration," ISO, Geneva.

[*14*] Stutts, D. S, Soedel, W., and Jha, S. K., "Fore-Aft Forces in Tire-Wheel Assemblies Generated by Unbalances and the Influence of Balancing," *Tire Science and Technology*, Vol. 19, 1991, pp. 142–162.

[*15*] Deodhar, A., "Ride Dynamic Response of Commercial Vehicles Subjected to Wheel Unbalance and Non-Uniformity Effects," M.Sc. Thesis, Concordia University, Montreal, 2005.

[*16*] Kenny, T., "Quantifying Tire, Rim and Vehicle Effects on Ride Quality," *SAE 890369*, SAE Warrendale, PA, 1989.

[*17*] Griffin, M. J., *Handbook of Human Vibration*, Elsevier Ltd., Southampton, UK, 1996.